

See discussions, stats, and author profiles for this publication at: <https://www.researchgate.net/publication/263982288>

Thermophysical Properties of Imidazolium-Based Lipidic Ionic Liquids

ARTICLE in JOURNAL OF CHEMICAL & ENGINEERING DATA · MAY 2013

Impact Factor: 2.04 · DOI: 10.1021/jc301004f

CITATIONS

4

READS

34

6 AUTHORS, INCLUDING:



Arsalan Mirjafari

Florida Gulf Coast University

44 PUBLICATIONS 271 CITATIONS

SEE PROFILE



Richard A. O'Brien

University of South Alabama

38 PUBLICATIONS 219 CITATIONS

SEE PROFILE



James H Davis

University of South Alabama

80 PUBLICATIONS 4,588 CITATIONS

SEE PROFILE



Kevin West

University of South Alabama

42 PUBLICATIONS 491 CITATIONS

SEE PROFILE

Thermophysical Properties of Imidazolium-Based Lipidic Ionic Liquids

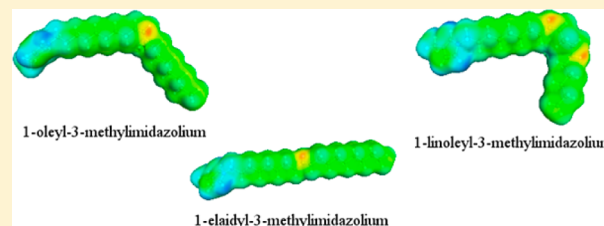
Samuel M. Murray,[†] T. Kyle Zimlich,[†] Arsalan Mirjafari,[‡] Richard A. O'Brien,[§] James H. Davis, Jr.,[§] and Kevin N. West^{*,†}

[†]Department of Chemical & Biomolecular Engineering and [§]Department of Chemistry, University of South Alabama

[‡]Department of Chemistry and Mathematics, Florida Gulf Coast University

S Supporting Information

ABSTRACT: The thermophysical properties of three lipidic ionic liquids, 1-oleyl-3-methylimidazolium bistriflimide, 1-elaidyl-3-methylimidazolium bistriflimide, and 1-linoleyl-3-methylimidazolium bistriflimide are measured at 1 bar as a function of temperature over the range of 273 K to 353 K and correlated to appropriate models. Each of these compounds is a variation on 1-C₁₈-3-methylimidazolium bistriflimide, where the C₁₈ chain contains one or more unsaturations, incorporated into the structure to lower the melting point. Derived properties such as molar volume and volume expansivity are also calculated. The data are compared with literature values for shorter chain 1-*n*-alkyl-3-methylimidazolium bistriflimide salts. The longer chains impart lower densities and higher viscosities relative to their shorter chain homologues. Although the subtle structural differences between the three compounds result in significant differences in melting points, there is less of an effect on the liquid phase thermophysical properties.



INTRODUCTION

In recent years, ionic liquids, molten salts with melting points lower than 100 °C, have gained great interest as process solvents for reactions and separations due to their often vanishingly low vapor pressures and the ability to tune their properties using structural modifications. Advances in their development have transitioned them from the first generation, where they were merely regarded as solvents, to a second generation of task-specific ionic liquids^{1,2} where functionalization of the cation or anion provides specific thermophysical or chemical properties designed to accomplish a specific reaction or separations task. Even now, a third generation of ionic liquids involving active pharmaceutical ingredients^{3,4} is being explored and developed.

Given the ionic nature of these species, they are often regarded as polar or moderately polar, although solvatochromic evidence points toward the more moderately polar end of the spectrum with hydrogen bonding ability highly dependent on cation and anion choice.⁵ Experimental measurements of inorganic salt solubility⁶ and hydrocarbon infinite dilution activity coefficients^{7–10} support the picture of these species being predominantly polar in nature. Though the properties of these species are highly tunable, no significant attempts had been made to design ionic liquids with nonpolar-like properties until recently. Likely, this was due to the widely known observation that for one of the most commonly employed cations, 1-alkyl-3-methylimidazolium, as the size of the *n*-alkyl chain in the 1 position is increased above ~9 carbons, the melting points begin to rise significantly, resulting in species that are room temperature solids.^{11–15}

Recently, our group demonstrated that by incorporating unsaturations into the *n*-alkyl chain the melting points of C₁₆–C₂₀ chain containing imidazolium bis(trifluoromethylsulfonyl)imide (bistriflimide) salts can be dramatically reduced, resulting in room temperature liquids with significant nonpolar content.¹⁶ This work was inspired by the behavior of natural lipids where species containing unsaturations have melting points significantly lower than their saturated counterparts. Because of this link to these naturally occurring compounds, the synthesis of the ionic liquids from precursors derived from fatty acids and their structural similarity to cationic lipids, we have named these species lipidic ionic liquids. Other researchers have demonstrated a similar phenomenon utilizing chain asymmetry through substitution on aryl rings in the chain.¹⁷

As part of further characterization of these novel species, we have measured the thermophysical properties (density, index of refraction, and dynamic viscosity) as a function of temperature at 1 bar for three representative lipidic ionic liquids described in our previous work. The names, nomenclature, and chemical formula of these species are shown in Table 1 along with their structures, melting points, and molar masses.

EXPERIMENTAL SECTION

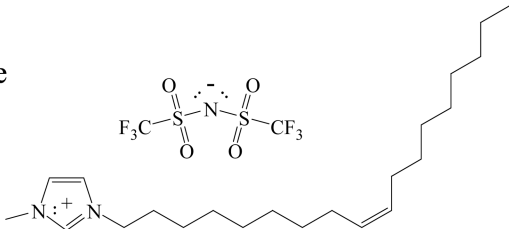
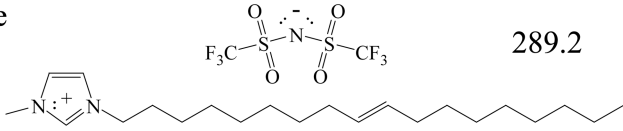
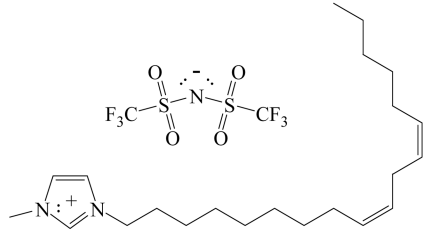
Chemicals. [Oleyl-mim][(CF₃SO₂)₂N], [elaidyl-mim][(CF₃SO₂)₂N], and [linoleyl-mim][(CF₃SO₂)₂N] were synthe-

Received: September 14, 2012

Accepted: May 15, 2013

Published: May 30, 2013

Table 1. Structures, Melting Points¹⁶ and Nomenclature of the Three Compounds Studied in This Work

Name, Nomenclature & Formula	Structure	Melting Point		MM g·mol ⁻¹
		K	°C	
1-(Z-octadec-9-enyl)-3-methylimidazolium bistriflimide [oleyl-mim][(CF ₃ SO ₂) ₂ N]		252.3	-20.9	613.72
C ₂₄ H ₄₁ F ₆ N ₃ O ₄ S ₂	CASRN: 1264476-00-7			
1-(E-octadec-9-enyl)-3-methylimidazolium bistriflimide [elaidyl-mim][(CF ₃ SO ₂) ₂ N]		289.2	16.0	613.72
C ₂₄ H ₄₁ F ₆ N ₃ O ₄ S ₂	CASRN: 1227922-96-4			
1-(Z,Z-octadec-9,12-dienyl)-3-methylimidazolium bistriflimide [linoleyl-mim][(CF ₃ SO ₂) ₂ N]		226.4	-46.8	611.70
C ₂₄ H ₃₉ F ₆ N ₃ O ₄ S ₂	CASRN: 1227922-98-6			

sized according to the methods outlined in our earlier work.¹⁶ Samples were stored under nitrogen and each sample was placed under vacuum (< 100 mbar) at 65 °C for at least 8 h immediately prior to making measurements to remove residual solvent, water, and dissolved gases that could evolve in the instruments as the temperature was increased. The samples were submitted to Galbraith Laboratories, Inc. for water and iodide impurity analysis and the results are shown in Table 2.

Density. Density measurements were made using an Anton Paar DSA 5000 vibrating tube densitometer. The densities of [oleyl-mim][(CF₃SO₂)₂N] and [linoleyl-mim][(CF₃SO₂)₂N] were measured in the temperature range from 273.15 K to 343.14 K (± 0.01 K); the density of [elaidyl-mim]-(CF₃SO₂)₂N was measured in the temperature range from

Table 2. Compound Source, Purity, And Impurity Analysis Methods. Synthesis Methods Reported in Our Earlier Paper.¹⁶

compound	source	mole fraction purity	analysis methods	H ₂ O content ^a	I ⁻ content ^a
[oleyl-mim] [(CF ₃ SO ₂) ₂ N]	synthesis	> 0.98	NMR/LCMS	< 0.23 %	< 0.34 %
[elaidyl-mim] [(CF ₃ SO ₂) ₂ N]	synthesis	> 0.98	NMR/LCMS	< 0.45 %	< 0.03 %
[linoleyl-mim] [(CF ₃ SO ₂) ₂ N]	synthesis	> 0.98	NMR/LCMS	< 0.22 %	< 0.02 %

^aH₂O and I⁻ analysis performed by Galbraith Laboratories, Inc. on 6/13/2012.

Table 3. Density (ρ) and Molar Volume (V) of [Oleyl-mim][$(\text{CF}_3\text{SO}_2)_2\text{N}$], [Elaidyl-mim][$(\text{CF}_3\text{SO}_2)_2\text{N}$] and [Linoleyl-mim][$(\text{CF}_3\text{SO}_2)_2\text{N}$] as Functions of Temperature (± 0.01 K) with Standard Uncertainty, u , Calculated Using a Relative Standard Uncertainty of 0.2 % Based on Purity of 98 %

T	[oleyl-mim] [$(\text{CF}_3\text{SO}_2)_2\text{N}$]			[elaidyl-mim] [$(\text{CF}_3\text{SO}_2)_2\text{N}$]			[linoleyl-mim] [$(\text{CF}_3\text{SO}_2)_2\text{N}$]		
	ρ	u	V	ρ	u	V	ρ	u	V
T/K	kg·m ⁻³	kg·m ⁻³	cm ³ ·mol ⁻¹	kg·m ⁻³	kg·m ⁻³	cm ³ ·mol ⁻¹	kg·m ⁻³	kg·m ⁻³	cm ³ ·mol ⁻¹
273.15	1211	2	506.8				1217	2	502.7
283.15	1203	2	510.3				1209	2	506.1
293.15	1194	2	513.8	1180	2	520.0	1201	2	509.5
303.15	1186	2	517.3	1172	2	523.6	1193	2	513.0
313.15	1178	2	520.8	1164	2	527.3	1184	2	516.4
323.15	1170	2	524.4	1156	2	531.0	1176	2	520.0
333.15	1162	2	527.9	1148	2	534.7	1169	2	523.4
343.15	1155	2	531.6	1140	2	538.4	1161	2	526.9

293.15 K to 343.15 K (± 0.01 K) as its melting point is 289 K. The densitometer was calibrated with Millipore quality water prior to and during measurements, with no detectable drift in accuracy.

Measurements were made by introducing the sample into the tube with a glass/PTFE syringe. The sample was then allowed to come to thermal equilibrium (as determined by the instrument) and the density was measured. Once a measurement was completed, the syringe plunger was advanced/retracted to displace 0.5–1.0 mL to allow a new portion of sample to enter the tube, providing a second, independent measurement which was made after temperature equilibration. This was repeated a third time, after which the temperature was changed for the next measurement and the process repeated. The reported values are the average of the three trials.

Refractive Index. Indices of refraction were measured on a ThermoFisher Scientific Abbe Refractometer in the temperature range 283.2 K to 343.2 K (± 0.1 K). At each temperature the instrument was calibrated using standards from Cargille Laboratories ($n_D = 1.4000, 1.4280, 1.4560$) and measurements were reproducible to within ± 0.0005 .

Dynamic Viscosity. Dynamic viscosity measurements were made using an Anton Paar AMVn microviscometer equipped with (1.6, 1.8, 3.0, and 4.0) mm glass capillary tubes, for varying viscosity ranges, using the rolling ball method. The steel ball and sample were loaded into the capillary tubes using the filling caps provided by the instrument manufacturer, ensuring no air bubbles were present in the tubes. The capillaries were then inserted into the temperature controlled rotor arm of the AMVn and allowed to come to thermal equilibrium. After the trials were completed, the temperature was changed and the process was repeated. For each temperature at least 40 trials (rolls of the ball) were recorded. The viscosity of [oleyl-mim][$(\text{CF}_3\text{SO}_2)_2\text{N}$] was measured in the temperature range from 278.15 K to 353.15 K (± 0.01 K); the viscosity of [elaidyl-mim][$(\text{CF}_3\text{SO}_2)_2\text{N}$] was measured in the temperature range from 293.15 K to 353.15 K (± 0.01 K); the viscosity of [linoleyl-mim][$(\text{CF}_3\text{SO}_2)_2\text{N}$] was measured in the temperature range from 280.15 K to 353.15 K (± 0.01 K). The viscosity was calculated using eq 1, where k_c is the capillary tube constant, t_r is the roll time, ρ_{ball} is the ball density, and ρ_{fluid} is the fluid density.

$$\mu \text{ (mPa}\cdot\text{s)} = k_c t_r (\rho_{\text{ball}} - \rho_{\text{fluid}}) \quad (1)$$

The reported values are the average of the trials.

RESULTS AND DISCUSSION

Density. The experimental data for the densities and the derived molar volumes of [oleyl-mim][$(\text{CF}_3\text{SO}_2)_2\text{N}$], [elaidyl-mim][$(\text{CF}_3\text{SO}_2)_2\text{N}$] and [linoleyl-mim][$(\text{CF}_3\text{SO}_2)_2\text{N}$] over the temperature range 273 K to 343 K are shown in Table 3 and the density data are shown graphically in Figure 1. The

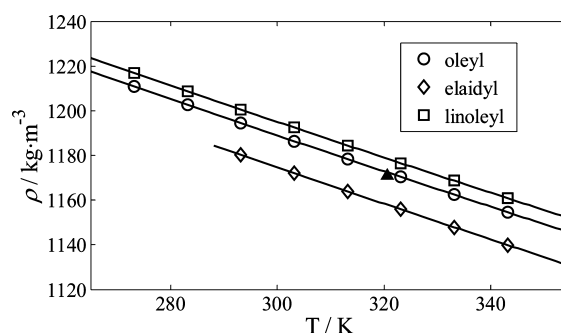


Figure 1. Density (ρ , kg·m⁻³) of (○) [oleyl-mim][$(\text{CF}_3\text{SO}_2)_2\text{N}$], (◇) [elaidyl-mim][$(\text{CF}_3\text{SO}_2)_2\text{N}$], and (□) [linoleyl-mim][$(\text{CF}_3\text{SO}_2)_2\text{N}$] as functions of temperature. The lines represent the least squared fit of eq 2. Additionally, the density of [oleyl-mim][$(\text{CF}_3\text{SO}_2)_2\text{N}$] at 320.6 K estimated from molecular dynamic simulations by Shah and Maginn²⁵ (▲) is shown.

densities of the compounds as functions of temperature were fit to a linear expression (eq 2) using a least-squares method. The fit parameters for the model as well as the R^2 values and standard deviations (eq 3) are shown in Table 4.

$$\rho \text{ (kg/m}^3\text{)} = a + bT(\text{K}) \quad (2)$$

$$s = \sqrt{\frac{1}{n_d - n_p} \sum_{i=1}^N \left(\frac{\rho_{\text{calc}} - \rho_{\text{exp}}}{\rho_{\text{exp}}} \right)^2} \quad (3)$$

As is typical, the densities of each compound decreases slightly with temperature, as the compounds are liquids far removed from their critical points. Although the slight structural variation in these compounds results in significant differences in their melting points, the effect on density is more subtle. [Elaidyl-mim][$(\text{CF}_3\text{SO}_2)_2\text{N}$] is the least dense followed by [oleyl-mim][$(\text{CF}_3\text{SO}_2)_2\text{N}$] and [linoleyl-mim][$(\text{CF}_3\text{SO}_2)_2\text{N}$], which contains two *cis*-double bonds, being the most dense. This phenomenon mimics that of molecular analogues where the midchain *cis*-bond results in marginally

Table 4. Coefficients for the Linear Fits of the Density (eqs 2) of [Oleyl-mim][(CF₃SO₂)₂N], [Elaidyl-mim][(CF₃SO₂)₂N], and [Linoleyl-mim][(CF₃SO₂)₂N] as a Function of Temperature, With the Standard Deviation from the Model As Calculated by eq 3

linear fit			
$a/\text{kg}\cdot\text{m}^{-3}$	$b/\text{kg}\cdot\text{m}^{-3}\cdot\text{K}^{-1}$	R^2	$s/\text{kg}\cdot\text{m}^{-3}$
[Oleyl-mim][(CF ₃ SO ₂) ₂ N]			
1430.3	-0.80398	0.999945	$1\cdot 10^{-4}$
[Elaidyl-mim][(CF ₃ SO ₂) ₂ N]			
1416.1	-0.80503	0.999979	$7\cdot 10^{-5}$
[Linoleyl-mim][(CF ₃ SO ₂) ₂ N]			
1435.3	-0.80043	0.999929	$1\cdot 10^{-4}$

higher densities than the *trans* isomer as is the case for the data compiled for 10 *cis/trans* alkene isomers in the work by Steele and Chirico.¹⁸

The difference in the densities between these three compounds, each of which contains a C₁₈ chain, is relatively small when compared to the densities of shorter chain 1-*n*-alkyl-3-methylimidazolium bistriflimide salts. In Figure 2, the

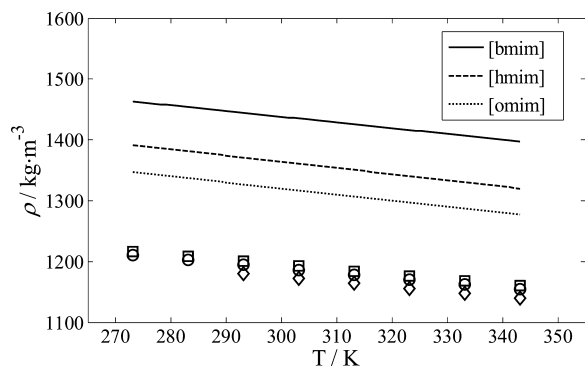


Figure 2. Comparison of the density of (○) [oleyl-mim][(CF₃SO₂)₂N], (◇) [elaidyl-mim][(CF₃SO₂)₂N] and (□) [linoleyl-mim][(CF₃SO₂)₂N] and shorter chain 1-*n*-alkyl-3-methylimidazolium bistriflimide salts: [bmim], 1-*n*-butyl-3-methylimidazolium bistriflimide; [hmim], 1-*n*-hexyl-3-methylimidazolium bistriflimide; [omim], 1-*n*-octyl-3-methylimidazolium bistriflimide.¹⁹

experimental densities of the three compounds studied in this work are shown along with the densities of the bistriflimide salts of 1-*n*-butyl-3-methylimidazolium ([bmim]), 1-*n*-hexyl-3-methylimidazolium ([hmim]), and 1-*n*-octyl-3-methylimidazolium ([omim]).¹⁹ The trend observed in the literature of decreasing density with increasing alkyl chain length is continued with these C₁₈ compounds. As the alkyl chain length increases, the lower density alkyl chain becomes a more significant volume fraction of the ionic liquid, thus lowering the density. Collectively, the three new data sets are representative of temperature-dependent density of a saturated C₁₈ chain compound, were it a liquid over the entire range.

The volume expansivities, α_p , of for each of the compounds have been calculated using eq 4 with the derivative quantity evaluated using the fit parameters for eq 2. The results are tabulated in Table 5 and shown graphically in Figure 3. While the volume expansivity for many ionic liquids has a negative slope with temperature,²⁰ the ionic liquids in this work exhibit a positive slope for α_p as a function of temperature, more akin to higher *n*-alkanes at low pressures.²¹ This is not surprising

Table 5. Volume expansivity (α_p) of [Oleyl-mim][(CF₃SO₂)₂N], [Elaidyl-mim][(CF₃SO₂)₂N] and [Linoleyl-mim][(CF₃SO₂)₂N] as Functions of Temperature (± 0.01 K)

T/K	[oleyl-mim] [(CF ₃ SO ₂) ₂ N]	[elaidyl-mim] [(CF ₃ SO ₂) ₂ N]	[linoleyl-mim] [(CF ₃ SO ₂) ₂ N]
	$\alpha_p\cdot 10^6/\text{K}^{-1}$	$\alpha_p\cdot 10^6/\text{K}^{-1}$	$\alpha_p\cdot 10^6/\text{K}^{-1}$
273.15	664.0		657.8
283.15	668.5		662.3
293.15	673.1	682.1	666.7
303.15	677.7	686.9	671.2
313.15	682.3	691.7	675.8
323.15	686.9	696.5	680.4
333.15	691.6	701.3	684.9
343.15	696.4	706.2	689.5

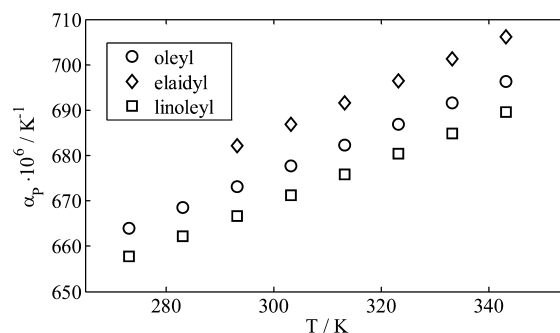


Figure 3. Volume expansivity (α_p) of (○) [oleyl-mim][(CF₃SO₂)₂N], (◇) [elaidyl-mim][(CF₃SO₂)₂N], and (□) [linoleyl-mim][(CF₃SO₂)₂N] as calculated by eq 4.

considering the significant volume fraction of these species that is occupied by the alkyl chain.

$$\alpha_p = -\frac{1}{\rho} \left(\frac{\partial \rho}{\partial T} \right)_p \quad (4)$$

Refractive Indices. The experimental data for the refractive indices of [oleyl-mim][(CF₃SO₂)₂N], [elaidyl-mim][(CF₃SO₂)₂N] and [linoleyl-mim][(CF₃SO₂)₂N] over the temperature range 283 to 343 K are shown in Table 6 and graphically in Figure 4. The refractive indices as functions of temperature were fit to a linear expression (eq 5) using a least-

Table 6. Refractive Indices (n_D) of [Oleyl-mim][(CF₃SO₂)₂N], [Elaidyl-mim][(CF₃SO₂)₂N], and [Linoleyl-mim][(CF₃SO₂)₂N] as Functions of Temperature (± 0.1 K) with the Standard Uncertainty, u , Based on Average Deviation from Calibration Standards at Each Temperature

T/K	[oleyl-mim] [(CF ₃ SO ₂) ₂ N]		[elaidyl-mim] [(CF ₃ SO ₂) ₂ N]		[linoleyl-mim] [(CF ₃ SO ₂) ₂ N]	
	n_D	u	n_D	u	n_D	u
283.2	1.4576	0.0005		0.0005	1.4710	0.0005
293.2	1.4545	0.0005	1.4510	0.0005	1.4676	0.0005
298.2	1.4528	0.0005	1.4493	0.0005	1.4661	0.0005
303.2	1.4511	0.0005	1.4476	0.0005	1.4645	0.0005
313.2	1.4479	0.0005	1.4443	0.0005	1.4612	0.0005
323.2	1.4446	0.0005	1.4410	0.0005	1.4580	0.0005
333.2	1.4410	0.0005	1.4374	0.0005	1.4547	0.0005
343.2	1.4379	0.0005	1.4343	0.0005	1.4517	0.0005

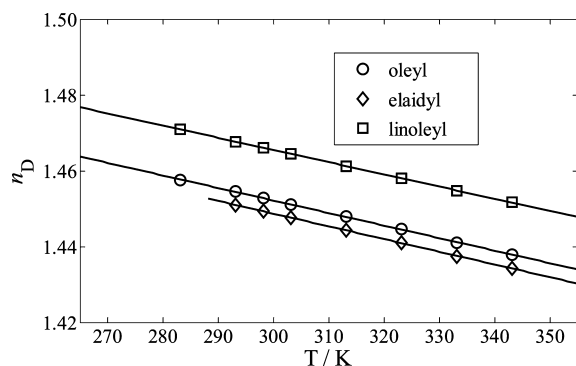


Figure 4. Refractive indices (n_D) of (○) [oleyl-mim][$(CF_3SO_2)_2N$], (◇) [elaïdyl-mim][$(CF_3SO_2)_2N$], and (□) [linoleyl-mim][$(CF_3SO_2)_2N$] as functions of temperature. The lines represent the least squared fit of eq 5.

squares method. The fit parameters for each compound as well as the R^2 values and standard deviations (eq 6) are shown in Table 7.

$$n_D = d_0 + d_1 T(K) \quad (5)$$

$$s = \sqrt{\frac{1}{n_d - n_p} \sum_{i=1}^N \left(\frac{n_{D,calc} - n_{D,exp}}{n_{D,exp}} \right)^2} \quad (6)$$

Table 7. Coefficients for the Linear Fits of the Refractive Indices (Equations X) of [Olelyl-mim][$(CF_3SO_2)_2N$], [Elaidyl-mim][$(CF_3SO_2)_2N$] and [Linoleyl-mim][$(CF_3SO_2)_2N$] as Function of Temperature, With the Standard Deviation from the Model As Calculated by eq 6

linear fit			
d_0	d_1	R^2	s
1.5514	$-3.3089 \cdot 10^{-4}$	0.99976	$8 \cdot 10^{-5}$
	[Olelyl-mim][$(CF_3SO_2)_2N$]		
1.5493	$-3.3536 \cdot 10^{-4}$	0.99982	$6 \cdot 10^{-5}$
	[Elaidyl-mim][$(CF_3SO_2)_2N$]		
1.5622	$-3.2225 \cdot 10^{-4}$	0.99986	$6 \cdot 10^{-5}$
	[Linoleyl-mim][$(CF_3SO_2)_2N$]		

As with similar compounds, the refractive index decreases with temperature in a manner similar to the density. Additionally, the refractive indices follow the same trend across the three compounds as does the density with [linoleyl-mim][$(CF_3SO_2)_2N$] having the highest index of refraction and [elaïdyl-mim][$(CF_3SO_2)_2N$] the lowest.

Dynamic Viscosity. The experimental data for the dynamic viscosities, η , of [oleyl-mim][$(CF_3SO_2)_2N$], [elaïdyl-mim][$(CF_3SO_2)_2N$] and [linoleyl-mim][$(CF_3SO_2)_2N$] over the temperature ranges of 278 K to 353 K, 293 K to 353 K, and 280 K to 353 K, respectively, are shown in Table 8 and graphically in Figure 5. The viscosities of the compounds as functions of temperature were fit to both an Arrhenius-type expression (eq 7) and the Vogel–Fulcher–Tamman (VFT) expression^{22–24} (eq 8) using a least-squares method. The fit parameters for each model as well as the R^2 values and standard deviations (eq 9) are shown in Table 9. An F -test comparing the models demonstrated that the three-parameter VFT model was statistically justified over the two-parameter Arrhenius model.

Table 8. Dynamic Viscosity (η) of [Olelyl-mim][$(CF_3SO_2)_2N$], [Elaidyl-mim][$(CF_3SO_2)_2N$], and [Linoleyl-mim][$(CF_3SO_2)_2N$] as Functions of Temperature (± 0.01 K) with Standard Uncertainty, u , Calculated as 1 % of Measured Values Based on the Accuracy of Calibration of the Instrument and Sample Purity

T/K	[oleyl-mim] [$(CF_3SO_2)_2N$]		[elaïdyl-mim] [$(CF_3SO_2)_2N$]		[linoleyl-mim] [$(CF_3SO_2)_2N$]	
	η /mPa·s	$\pm u$	η /mPa·s	$\pm u$	η /mPa·s	$\pm u$
278.15	1005.3	10				
280.15					756	8
283.15	699	7			632	6
288.15	493	5			452	5
293.15	356	4	370	4	332	3
298.15	264	3	274	3	248	2
303.15	223	2	224	2	181	2
313.15	133.9	1.3	133.8	1.3	112.1	1.1
323.15	86.0	0.9	85.3	0.9	73.7	0.7
333.15	58.1	0.6	57.4	0.6	50.9	0.5
343.15	41.1	0.4	40.4	0.4	36.7	0.4

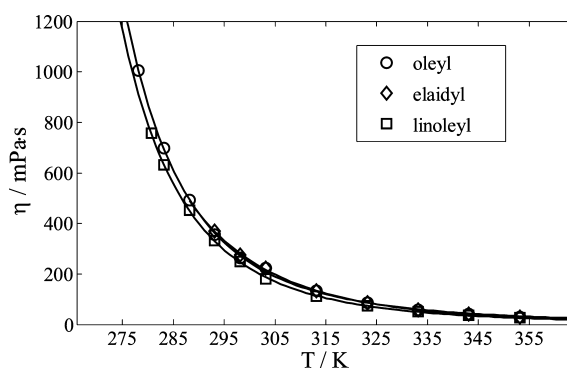


Figure 5. Dynamic viscosities (η , mPa·s) of (○) [oleyl-mim][$(CF_3SO_2)_2N$], (◇) [elaïdyl-mim][$(CF_3SO_2)_2N$], and (□) [linoleyl-mim][$(CF_3SO_2)_2N$] as functions of temperature. The lines represent the least squared fit of eq 8.

$$\eta \text{ (mPa·s)} = \eta_{\infty} \exp\left(\frac{-E_a}{RT}\right) \quad (7)$$

$$\eta \text{ (mPa·s)} = A \exp\left(\frac{k}{T - T_0}\right) \quad (8)$$

$$s = \sqrt{\frac{1}{n_d - n_p} \sum_{i=1}^N \left(\frac{\eta_{calc} - \eta_{exp}}{\eta_{exp}} \right)^2} \quad (9)$$

For many ionic liquids, viscosity is a strong function of temperature near room temperature, as is the case for these compounds, with viscosities varying over 3 orders of magnitude in the temperature range studied. The three compounds exhibit a low diversity in their viscosities, as with their densities, with [oleyl-mim][$(CF_3SO_2)_2N$] and [elaïdyl-mim][$(CF_3SO_2)_2N$] having almost identical viscosities at higher temperatures and [linoleyl-mim][$(CF_3SO_2)_2N$] exhibiting a slightly lower viscosity over the temperature range studied. Thus, it appears that, as with density, the orientation of the double bond and the inclusion of a second double bond in the chain have little influence on the viscosity, whereas they have a significant

Table 9. Coefficients for the Arrhenius and VFT models (eqs 7 and 8, respectively) of [Oleyl-mim][(CF₃SO₂)₂N], [elaidyl-mim][(CF₃SO₂)₂N], and [linoleyl-mim][(CF₃SO₂)₂N] as a function of temperature, with the model standard deviation as calculated by eq 9

Arrhenius model			VFT model					
$\eta_{\infty}/\text{mPa}\cdot\text{s}$	$E_a/\text{kJ}\cdot\text{mol}^{-1}$	R^2	$s/\text{mPa}\cdot\text{s}$	$A/\text{mPa}\cdot\text{s}$	k/K	T_0/K	R^2	$s/\text{mPa}\cdot\text{s}$
[Oleyl-mim][(CF ₃ SO ₂) ₂ N]								
$4.97\cdot 10^{-6}$	-44.19	0.9974	0.2	0.263	875.15	172.08	0.9996	0.05
[Elaidyl-mim][(CF ₃ SO ₂) ₂ N]								
$6.54\cdot 10^{-5}$	-37.87	0.9989	0.1	$6.51\cdot 10^{-3}$	2155.87	96.14	0.9991	0.02
[Linoleyl-mim][(CF ₃ SO ₂) ₂ N]								
$5.82\cdot 10^{-6}$	-43.56	0.9989	0.2	$6.23\cdot 10^{-2}$	1212.41	151.72	0.9999	0.03

influence on melting point. Again, this trend can be observed in alkene molecular analogues of these compounds.

In Figure 6 the viscosities of the three studied compounds are plotted along with the viscosities of the shorter chain 1-*n*-

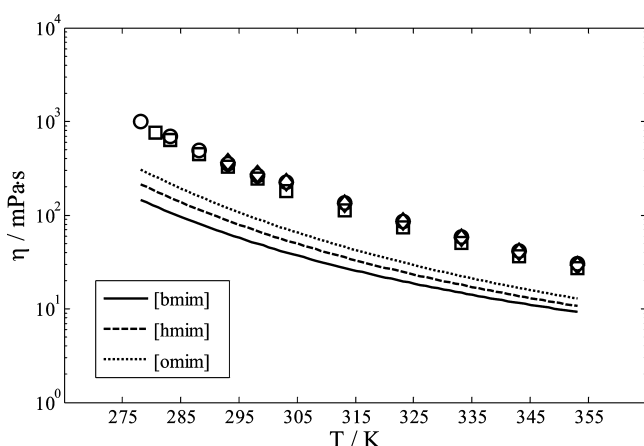


Figure 6. Comparison of the dynamic viscosities of (○) [Oleyl-mim][(CF₃SO₂)₂N], (◇) [Elaidyl-mim][(CF₃SO₂)₂N], and (□) [Linoleyl-mim][(CF₃SO₂)₂N] and shorter chain 1-alkyl-3-methylimidazolium bistriflimide salts: [bmim], 1-*n*-butyl-3-methylimidazolium bistriflimide; [hmim], 1-*n*-hexyl-3-methylimidazolium bistriflimide; [omim], 1-*n*-octyl-3-methylimidazolium bistriflimide.¹⁹

alkyl-3-methylimidazolium bistriflimide salts, 1-*n*-butyl-3-methylimidazolium ([bmim]), 1-*n*-hexyl-3-methylimidazolium ([hmim]), and 1-*n*-octyl-3-methylimidazolium ([omim]).¹⁹ In the context of this series, the length of the alkyl chain continues to play a significant role in determining viscosity, with longer chain species exhibiting higher viscosities due to increased dispersion force interactions. Compared with their shorter chain homologues, the viscosities of the three new compounds all fall within a narrow window that would seem to be representative of C₁₈ containing homologues with subtle structural variation.

CONCLUSIONS

In this work we studied the thermophysical properties of three 1-C₁₈-3-methylimidazolium bistriflimide salts that differ only in the number and orientation of double bonds in their structure which were introduced to lower melting points relative to the saturated chain homologue. The density, refractive index and dynamic viscosity have been measured as functions of temperature and fit to appropriate models and the molar volume and volume expansivity has been calculated from the temperature dependent density data.

The subtle structural changes that led to significant differences in melting points have a much smaller effect on the liquid phase thermophysical properties of the three lipidic ionic liquids studied. Although small, differences in density can be attributed to polarity differences between *cis*- and *trans*-double bonds. Trends in the refractive indices parallel those of density. The viscosities of the two compounds containing a single double bond in the alkyl chain (*cis*- vs *trans*-) were almost identical, while the compound with two *cis*-double bonds in the chain had a slightly lower viscosity. When compared with shorter chain analogues, the density and viscosity trends as function of alkyl chain length are continued with lower densities and higher viscosities for the C₁₈ species, representative of values expected for a saturated C₁₈ chain, were it a liquid over the entire temperature range.

All of the thermophysical properties measured herein point to species with similar properties to their short chain homologues, but property trends consistent with significantly longer alkyl chains. Sufficiently long alkyl chains should impart nonpolar character to these ionic liquids, allowing them to be used for processes involving nonpolar species that are not presently possible with conventional ionic liquids. Currently, we are studying the binary multicomponent phase equilibria of these and other lipidic ionic liquids with both polar and nonpolar molecular species to probe where these species can be used for reactions and separations involving nonpolar species.

ASSOCIATED CONTENT

Supporting Information

Graphical representation of the deviations between the model and experimental values for the properties discussed. This material is available free of charge via the Internet at <http://pubs.acs.org>.

AUTHOR INFORMATION

Corresponding Author

*E-mail: kevinwest@southalabama.edu. Tel.: 251-460-7563. Address: University of South Alabama 150 Jaguar Drive Mobile, AL 36688.

Funding

K.N.W. and J.H.D. wish to thank the National Science Foundation for support of this work (NSF CBET Award No. 1133101).

Notes

The authors declare no competing financial interest.

REFERENCES

- (1) Davis, J. H., Jr. Task-Specific Ionic Liquids. *Chem. Lett.* **2004**, *33*, 1072–1077.

- (2) Davis, J. H.; Wasserscheid, P. *Synthesis of Task-Specific Ionic Liquids*; Wiley-VCH: Berlin, 2008; pp 45–55.
- (3) Bica, K.; Shamshina, J.; Hough, W. L.; MacFarlane, D. R.; Rogers, R. D. Liquid forms of pharmaceutical co-crystals: Exploring the boundaries of salt formation. *Chem. Commun.* **2011**, 47, 2267–2269.
- (4) Elliott, G. D.; Kemp, R.; MacFarlane, D. R. The development of ionic liquids for biomedical applications—Prospects and challenges. *ACS Symp. Ser.* **2009**, 1030, 95–105.
- (5) Hallett, J. P.; Welton, T. How polar are ionic liquids? *ECS Trans.* **2009**, 16, 33–38.
- (6) Pereira, A. B.; Araujo, J. M. M.; Oliveira, F. S.; Esperanca, J. M. S. S.; Canongia, L. J. N.; Marrucho, I. M.; Rebelo, L. P. N. Solubility of inorganic salts in pure ionic liquids. *J. Chem. Thermodyn.* **2012**, 55, 29–36.
- (7) Deenadayalu, N.; Letcher, T. M.; Reddy, P. Determination of Activity Coefficients at Infinite Dilution of Polar and Nonpolar Solutes in the Ionic Liquid 1-Ethyl-3-methylimidazolium Bis-(trifluoromethylsulfonyl) Imide Using Gas-Liquid Chromatography at the Temperature 303.15 or 318.15 K. *J. Chem. Eng. Data* **2005**, 50 (1), 105–108.
- (8) Ge, M.-L.; Wang, L.-S.; Li, M.-Y.; Wu, J.-S. Activity Coefficients at Infinite Dilution of Alkanes, Alkenes, and Alkyl Benzenes in 1-Butyl-3-methylimidazolium Trifluoromethanesulfonate Using Gas-Liquid Chromatography. *J. Chem. Eng. Data* **2007**, 52 (6), 2257–2260.
- (9) Heintz, A.; Casas, L. M.; Nesterov, I. A.; Emel'yanenko, V. N.; Verevkin, S. P. Thermodynamic Properties of Mixtures Containing Ionic Liquids. 5. Activity Coefficients at Infinite Dilution of Hydrocarbons, Alcohols, Esters, and Aldehydes in 1-Methyl-3-butylimidazolium Bis(trifluoromethyl-sulfonyl) Imide Using Gas-Liquid Chromatography. *J. Chem. Eng. Data* **2005**, 50 (5), 1510–1514.
- (10) Yang, X.-J.; Wu, J.-S.; Ge, M.-L.; Wang, L.-S.; Li, M.-Y. Activity coefficients at infinite dilution of alkanes, alkenes, and alkyl benzenes in 1-hexyl-3-methylimidazolium trifluoromethanesulfonate using gas-liquid chromatography. *J. Chem. Eng. Data* **2008**, 53 (5), 1220–1222.
- (11) Bradley, A. E.; Hardacre, C.; Holbrey, J. D.; Johnston, S.; McMath, S. E. J.; Nieuwenhuyzen, M. Small-Angle X-ray Scattering Studies of Liquid Crystalline 1-Alkyl-3-methylimidazolium Salts. *Chem. Mater.* **2002**, 14, 629–635.
- (12) Dzyuba, S. V.; Bartsch, R. A. Influence of Structural Variations in 1-Alkyl(aralkyl)-3-methylimidazolium Hexafluorophosphates and Bis(Trifluoromethyl-Sulfonyl)Imides on Physical Properties of the Ionic Liquids. *ChemPhysChem* **2002**, 3, 161–166.
- (13) Gordon, C. M.; Holbrey, J. D.; Kennedy, A. R.; Seddon, K. R. Ionic Liquid Crystals: Hexafluorophosphate Salts. *J. Mater. Chem.* **1998**, 8, 2627–2636.
- (14) Holbrey, J. D.; Seddon, K. R. The Phase Behaviour of 1-Alkyl-3-methylimidazolium Tetrafluoroborates; Ionic Liquids and Ionic Liquid Crystals. *J. Chem. Soc., Dalton Trans.* **1999**, 2133–2140.
- (15) Lopez-Martin, I.; Burello, E.; Davey, P. N.; Seddon, K. R.; Rothenberg, G. Anion and Cation Effects on Imidazolium Salt Melting Points: A Descriptor Modelling Study. *ChemPhysChem* **2007**, 8, 690–695.
- (16) Murray, S. M.; O'Brien, R. A.; Mattson, K. M.; Ceccarelli, C.; Sykora, R. E.; West, K. N.; Davis, J. H., Jr. The Fluid-Mosaic Model, Homeoviscous Adaptation, and Ionic Liquids: Dramatic Lowering of the Melting Point by Side-Chain Unsaturation. *Angew. Chem., Int. Ed.* **2010**, 49, 2755–2758.
- (17) Ahrens, S.; Peritz, A.; Strassner, T. Tunable Aryl Alkyl Ionic Liquids (TAAILs): The Next Generation of Ionic Liquids. *Angew. Chem., Int. Ed.* **2009**, 48, 7908–7910.
- (18) Steele, W. V.; Chirico, R. D. Thermodynamic Properties of Alkenes (Mono-olefins Larger than C₄). *J. Phys. Chem. Ref. Data* **1993**, 22, 377–430.
- (19) Tokuda, H.; Hayamizu, K.; Ishii, K.; Susan, M. A. B. H.; Watanabe, M. Physicochemical Properties and Structures of Room Temperature Ionic Liquids. 2. Variation of Alkyl Chain Length in Imidazolium Cation. *J. Phys. Chem. B* **2005**, 109, 6103–6110.
- (20) Gu, Z.; Brennecke, J. F. Volume Expansivities and Isothermal Compressibilities of Imidazolium and Pyridinium-Based Ionic Liquids. *J. Chem. Eng. Data* **2002**, 47 (2), 339–345.
- (21) Navia, P.; Troncoso, J.; Romani, L. Isobaric Thermal Expansivity for Nonpolar Compounds. *J. Chem. Eng. Data* **2010**, 55, 2173–2179.
- (22) Fulcher, G. S. Analysis of recent measurements of the viscosity of glasses. *J. Am. Ceram. Soc.* **1925**, 8, 339–355.
- (23) Tammann, G.; Hesse, W. Die Abhängigkeit der Viskosität von der Temperatur bei unterkühlten flüssigkeiten (The dependence of the viscosity on temperature for super-cooled liquids). *Z. Anorg. Allg. Chem.* **1926**, 156, 245–257.
- (24) Vogel, H. Das Temperaturabhängigkeitsgesetz der Viskosität von Flüssigkeiten (The temperature dependence of the viscosity of liquids). *Phys. Z.* **1921**, 22, 645–646.
- (25) Shah, J. K.; Maginn, E. J. Molecular dynamics investigation of biomimetic ionic liquids. *Fluid Phase Equilib.* **2010**, 294, 197–205.